2022 American Control Conference (ACC)
Atlanta, USA, June 8-10, 2022

Swirling Pendulum Dynamics and Control: A Pedagogical Perspective

Shubhankar Riswadkar, Jaydeep Kakadiya, Sujay D. Kadam, Karanbir Sidhu and Harish J. Palanthandalam-Madapusi,
SysIDEA Robotics Lab, IIT Gandhinagar, India.

***Abstract*— The swirling pendulum is an underactuated, two-link, two-degree-of-freedom mechanism consisting of a pair of swirling and swinging links, that on account of its unusual out-of-the plane inertial coupling exhibits interesting dynamics and dynamical properties like multiple (eight) isolated equilibria (both stable as well as unstable), regions with loss of relative degree, loss of controllability and loss of inertial coupling. This work is an attempt to highlight the utility of the swirling pendulum as an attractive as well as a simple system for demonstrating a range of concepts/notions a learner would typically encounter in academic courses related to controls and dynamics. To achieve this goal, we start by presenting a (yet incomplete) summary of modeling, analysis, and control design concepts that can be studied in linear or nonlinear frameworks in various courses. We discuss as examples, the problems of input-output linearization and partial feedback linearization picked up from this summary. Furthermore, we also present inversion-based selective tracking control for tracking trajectories on the swirling pendulum outputs. In doing so, we explain how the problem of system zeros on the imaginary axis (that results in an unstable inversion-based feedforward controller) is avoided. We conclude by mentioning the problems that can be taken up as future work.**

I. Introduction

The swirling pendulum introduced in [1] is a two link mechanism having two degrees of freedom. The two links of the swirling pendulum are connected in an L-shaped manner as shown in Fig. 1. One of the link (blue) connected to a support at the fixed end performs a swinging motion like a simple pendulum. To the free end of this swinging link, is a second link (orange) connected such that it is perpendicular to the swinging link and is free to swirl around the point of connection (with the axis of swirl rotation along the first link). The swirling motion of the second link produces a swinging motion in the first link. The dynamics of the swinging link and the dynamics of the swirling link are coupled, and the inertial coupling between the two leads to a rich set of dynamic properties/behavior exhibited by the swirling pendulum, as will be seen subsequently. The two links are connected at an angle perpendicular to each other for simplicity. However it is possible to consider a different angle so that the links are connected to each other non-perpendicularly and still perform the motions described earlier. The swirling link is actuated and a torque can be applied to set the link in motion. However, the swinging link is not actuated, making the swirling pendulum an underactuated mechanical system. Furthermore, it is worth noting that the task space of the swirling pendulum is non-planar and the locus of the end point of the swirling link is three dimensional, since the motion of swirling link is not restricted to the plane of the swinging link.

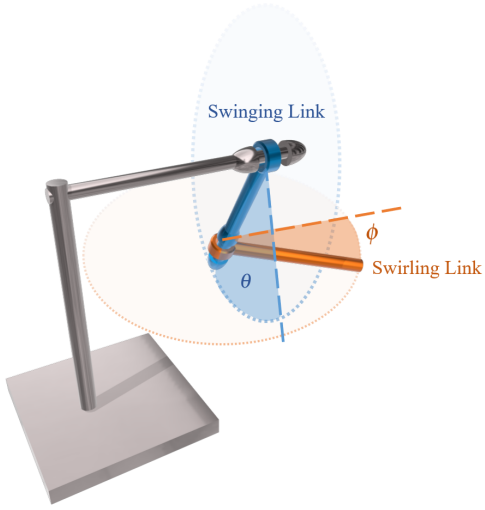

Fig. 1. A 3D rendered schematic diagram of the swirling pendulum shows two links - the swinging link (blue) and the swirling link (orange) connected to a support. The swinging link performs a motion similar to a simple pendulum by rotating about the fixed end and the swirling link connected perpendicularly to the open end of the swinging link and 'swirls' around this open end with the axis of the swirl rotation being along the swinging link

It is interesting to note that the swirling pendulum also exhibits multiple (eight) static equilibria, both stable as well as unstable. Also, in a certain configuration of the links, that also contains a few of the equilibrium points, we observe loss of inertial coupling, loss of controllability/actuation and loss of relative degree. This happens when swirling link is in the same plane as that of the swinging link plane. It would be worth noting that there exist two distinct and disconnected regions in the task space of the swirling pendulum within which equilibria under presence of torque can be defined. All these peculiar properties and behavior of the swirling pendulum along with its mathematical simplicity make the swirling pendulum an attractive platform for researchers and learners alike in systems and control, dynamics, and robotics. Other mechanisms similar to the swirling pendulum that have received a lot of attention in the literature are the acrobot [2], pendubot [3], Furuta pendulum [4], inverted pendulum/pole-on-a-cart [5], and the inertia wheel pendulum [6] mechanisms.

As will be seen in the following sections, the swirling pendulum offers a wide range of problems/challenges or concepts pertinent from both academic research and academic teaching point of view [1]. We present in this work the pedagogical utility that the swirling pendulum as a single system brings in for classroom teaching/learning of several

978-1-6654-5196-3/$31.00 ©2022 AACC

concepts in control and dynamics courses at different levels as elaborated next. The single-input single-output (SISO) or multi-input multi-output (MIMO) linearized systems (see Appendix of [1]) derived from swirling pendulum dynamics serve as an excellent classroom/coursework example for explaining both classical and modern control tools/methods like frequency domain analysis, compensate design, state space methods based analysis and control design, stability analysis and control synthesis for stabilization and trajectory tracking [1]. Owing to its rich set of properties, highly local behavior around the various equilibria, and underactuated nature, it also serves as an excellent example for nonlinear control problems and geometric control problems. It is possible to build the swirling pendulum hardware setup catering to different levels of sophistication - from a coursework assignment to a capstone project. The objective of this work is to highlight the swirling pendulum mechanism as a simple but attractive academic/coursework problem that serves to demonstrate several ideas or notions a learner would encounter in a controls oriented course and at different levels, while keeping a balance between complexity of the swirling pendulum system and its utility in explaining concepts in control. Towards this, we first present in Table I, a (not exhaustive or complete) summary of modeling, analysis and control concepts in which the swirling pendulum can be used to explain in linear or nonlinear frameworks and in a classical, modern or advanced coursework setting.

We present initially for the swirling pendulum governing equations in the manipulator form and the nonlinear affine-in-control form, pertinent from the point of robotics/control theory and later comment about the equilibrium points and their stability. We pick the problem of feedback linearization and demonstrate results for collocated and non-collocated partial feedback linearization, and input-output linearization of the swirling pendulum to show that a part of the nonlinear dynamics can be cancelled out and an auxiliary control input can be used to perform tracking on desired trajectories. In our second contribution, we derive the normal form equations and the zero dynamics for the swirling pendulum. Towards the end of the paper, in our third contribution, we discuss the inversion based-control for tracking desired trajectories. Inversion based-control in case of the swirling pendulum presents the peculiar challenge of presence of system zeros on imaginary axis, which is addressed by making use of selective or prioritized tracking [7]. Finally, we conclude by mentioning control problems that can be taken up as future work using the swirling pendulum.

II. Equations of Motion, Equilibrium Points and Stability

In this section we recall from an earlier work [1] the equations of motion for the swirling pendulum, its equilibrium points and their stability for the convenience of the reader. The equations of motion for the swirling pendulum in manipulator form are written as

$$\mathbf{M}(q)\ddot{q}+\mathbf{C}(q,\dot{q})\dot{q}+\mathbf{G}(q)=\mathbf{B}\tau, \tag{1}$$

where $q \triangleq \begin{bmatrix}\theta\\ \phi\end{bmatrix}$ is the vector of chosen generalized co-ordinates θ and ϕ are as indicated in the schematic diagram in Fig. 1, $\mathbf{M}(q) \in \mathbb{R}^{2\times 2}$, $\mathbf{C}(q,\dot{q}) \in \mathbb{R}^{2\times 2}$, $\mathbf{G}(q) \in \mathbb{R}^{2\times 1}$ and $\mathbf{B} \in \mathbb{R}^{2\times 1}$. Furthermore, $\mathbf{M}_{11} = \frac{4}{3}\left(m_1\ell_1^2+m_2(3\ell_1^2+\ell_2^2\sin^2\phi)\right)$, $\mathbf{M}_{12} = \mathbf{M}_{21} = 2m_2\ell_1\ell_2\cos\phi$, $\mathbf{M}_{22} = \frac{4}{3}m_2\ell_2^2$, $\mathbf{C}_{11} = \frac{4}{3}m_2\ell_2^2\sin\phi\cos\phi\dot{\phi}$, $\mathbf{C}_{12} = \frac{4}{3}m_2\ell_2^2\sin\phi\cos\phi\dot{\theta} - 2m_2\ell_1\ell_2\sin\phi\dot{\phi}$, $\mathbf{C}_{21} = -\frac{4}{3}m_2\ell_2^2\cos\phi\sin\phi\dot{\theta}$, $\mathbf{C}_{22} = 0$, $\mathbf{G}_1 = (m_1+2m_2)g\ell_1\sin\theta + m_2g\ell_2\sin\phi\cos\theta$, $\mathbf{G}_2 = m_2g\ell_2\sin\theta\cos\phi$, $\mathbf{B}_1 = 0$ and $\mathbf{B}_2 = 1$. Torque τ is applied on the swirling link such that it changes angle ϕ and can only change θ through inertial coupling between the two links. In the paper, all angular positions, velocities, accelerations and torques are functions of time and are written without the detail of (t) in the notation for simplicity. Also, m_1, m_2 denote respective link masses, ℓ_1, ℓ_2 denote respective link lengths and g denotes the acceleration due to gravity.

Remark 2.1: It is worth noting that for $k \in \mathbb{Z}\backslash\{0\}$, $\cos\frac{\pi}{2}k = 0$, and $\mathbf{M}_{12} = \mathbf{M}_{21} = 0$, meaning that inertial coupling between the two links is lost for these values of ϕ.

For the numerical and simulation results presented in the paper, we use the parameter values given in Table II.

The potential energy of the swirling pendulum is given by $\mathbf{P} \triangleq m_2g\ell_2\sin\phi\sin\theta - 2m_2g\ell_1\cos\theta - m_1g\ell_1\cos\theta$ and equilibrium points of the system are all the points q that satisfy $\frac{\partial\mathbf{P}}{\partial q} = \begin{bmatrix}(m_1+2m_2)gl_1\sin\theta+m_2gl_2\sin\phi\cos\theta\\ m_2gl_2\sin\theta\cos\phi\end{bmatrix} = 0$. These points are depicted in the Figure 2. These equilibrium points are periodic with respect to θ and ϕ and we can identify the eight equilibrium points within the interval $[-\pi\ \ \pi]$ as $\begin{bmatrix}0\\0\end{bmatrix}, \begin{bmatrix}0\\\pi\end{bmatrix}, \begin{bmatrix}\tilde{\theta}_e\\-\frac{\pi}{2}\end{bmatrix}, \begin{bmatrix}-\tilde{\theta}_e\\\frac{\pi}{2}\end{bmatrix}, \begin{bmatrix}\pi\\0\end{bmatrix}, \begin{bmatrix}\pi\\\pi\end{bmatrix}, \begin{bmatrix}(\pi-\tilde{\theta}_e)\\\frac{\pi}{2}\end{bmatrix}, \begin{bmatrix}(\pi+\tilde{\theta}_e)\\-\frac{\pi}{2}\end{bmatrix}$, where $\tilde{\theta}_e \triangleq \tan^{-1}\left(\frac{m_2l_2}{2m_2l_1+m_1l_1}\right)$. It is interesting to note that except $\begin{bmatrix}\tilde{\theta}_e\\-\frac{\pi}{2}\end{bmatrix}, \begin{bmatrix}-\tilde{\theta}_e\\\frac{\pi}{2}\end{bmatrix}$, all the remaining equilibrium points are unstable, including two hanging unstable equilibria (!) this is verified by checking at the eigenvalue signs of the matrix $\frac{\partial^2\mathbf{P}}{\partial q^2}$.

The swirling pendulum equations of motion can be expressed in the nonlinear affine-in-control form as,

$$\dot{x} = \mathbf{f}(x)+\mathbf{g}(x)u \tag{2}$$

where the state x is defined as

$$x \triangleq \begin{bmatrix}\theta\ \ \phi\ \ \dot{\theta}\ \ \dot{\phi}\end{bmatrix}^T, \tag{3}$$

and

$$\mathbf{f}(x) = \begin{bmatrix}\dot{\theta}\\ \dot{\phi}\\ -\overline{\mathbf{M}}_{11}^{-1}\overline{\mathbf{G}}_1-\overline{\mathbf{M}}_{11}^{-1}\overline{\mathbf{C}}_{12}\dot{\phi}-\overline{\mathbf{M}}_{11}^{-1}\overline{\mathbf{C}}_{11}\dot{\theta}\\ \mathbf{M}_{22}^{-1}\overline{\mathbf{G}}_2+\mathbf{M}_{22}^{-1}\overline{\mathbf{C}}_{22}\dot{\phi}+\mathbf{M}_{22}^{-1}\overline{\mathbf{C}}_{21}\dot{\theta}\end{bmatrix}, \mathbf{g}(x) = \begin{bmatrix}0\\0\\-\overline{\mathbf{M}}_{11}^{-1}\mathbf{M}_{12}\mathbf{M}_{22}^{-1}\\ \mathbf{M}_{22}^{-1}\overline{\mathbf{M}}_{22}\end{bmatrix}. \tag{4}$$

Note that, $\overline{\mathbf{M}}_{11} = \mathbf{M}_{11} - \mathbf{M}_{12}{\mathbf{M}_{22}}^{-1}\mathbf{M}_{21}$, $\overline{\mathbf{C}}_{11} = \mathbf{C}_{11} - \mathbf{M}_{12}{\mathbf{M}_{22}}^{-1}\mathbf{C}_{21}$, $\overline{\mathbf{C}}_{12} = \mathbf{C}_{12} - \mathbf{M}_{12}{\mathbf{M}_{22}}^{-1}\mathbf{C}_{22}$, $\overline{\mathbf{G}}_1 = \mathbf{G}_1 - \mathbf{M}_{12}{\mathbf{M}_{22}}^{-1}\mathbf{G}_2$, $\overline{\mathbf{M}}_{22} = 1 + \mathbf{M}_{21}{\overline{\mathbf{M}}_{11}}^{-1}\mathbf{M}_{12}{\mathbf{M}_{22}}^{-1}$, $\overline{\mathbf{G}}_2 = \mathbf{M}_{21}{\overline{\mathbf{M}}_{11}}^{-1}\overline{\mathbf{G}}_1 - \mathbf{G}_2$, $\overline{\mathbf{C}}_{22} = \mathbf{M}_{21}{\overline{\mathbf{M}}_{11}}^{-1}\overline{\mathbf{C}}_{12} - \mathbf{C}_{22}$, and $\overline{\mathbf{C}}_{21} = \mathbf{M}_{21}{\overline{\mathbf{M}}_{11}}^{-1}\overline{\mathbf{C}}_{11} - \mathbf{C}_{21}$.

TABLE I

SOME CONCEPTS IN SYSTEMS AND CONTROL THAT MAY BE STUDIED IN A COURSEWORK OR A PROJECT COURSE USING SWIRLING PENDULUM

		Linear Systems Framework		Nonlinear Systems Framework
		SISO	MIMO	SISO or MIMO
Modeling	Classiscal	Transfer function (matrix) - continuous or discrete		Lagrangian, Hamiltonian formulation
	Modern	State-space formulation (continuous or discrete)		
Analysis	Classiscal	Classical time and frequency domain analysis, stability analysis through root locus, Routh-Hurwitz criterion, Jury's stability test (discrete-time)	Matrix fraction descriptions	Stability analysis based on Lyapunov methods
	Modern	Controllability and observability analysis, stability analysis, Multivariable and invariant zeros		Feedback linearization: partial feedback and input-output feedback linearization, zero dynamics and normal form equations, Nonlinear controllability analysis
Control	Classical	P/PD/PI/PID Control, compensator design using classical tools of analysis	Master-Slave control	Computed Torque Control, PD control
	Modern	Inversion-based control, variable structure control, state/output feedback control, observer design/observer based control		Passivity based control, Inversion-based control, variable structure control, state/output feedback control, observer design/observer based control
	Advanced	Geometric control, adaptive control, Energy injection based swing-up and stabilization , Reinforcement and machine learning control		

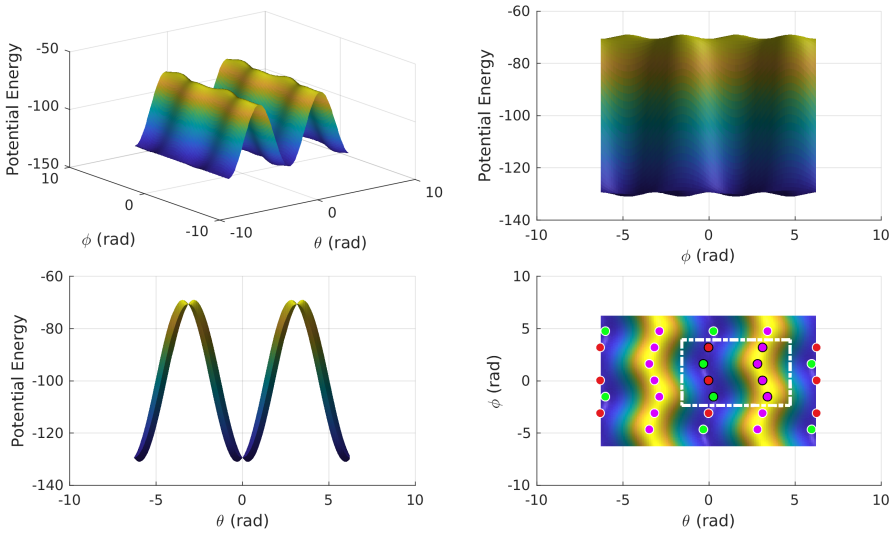

Fig. 2. Plots show the potential energy surface changing with respect to generalized coordinates. Equilibrium points of the swirling pendulum system are mapped on the surface and are periodic with respect to the generalized coordinates and potential energy. The eight unique equilibria are shown in the bottom right panel in an enclosed box with their periodic copies. These eight equilibria include two stable (green) and six unstable (magenta and red) equilibria including two hanging (!) unstable equilibria (red).

TABLE II

PARAMETER VALUES FOR THE SWIRLING PENDULUM

m_1	m_2	ℓ_1	ℓ_2	g
0.435 kg	0.325 kg	0.07 m	0.0855 m	9.81 m/s^2

III. ON THE FEEDBACK LINEARIZATION OF SWIRLING PENDULUM

In this section we discuss the feedback linearization of the swirling pendulum using partial feedback and input-output feedback linearization. It is worth noting that since swirling pendulum an underactuated system, it can only be partially linearized using a feedback.

A. Input-Output Linearization

In this subsection, we explore linearization of input-output dynamics making use of dynamic state feedback, choosing θ as output. Letting $y \triangleq \mathbf{h}(x) = [1\ 0\ 0\ 0]x = \theta$, we have

$$\dot{y} = \frac{\partial \mathbf{h}}{\partial x}\dot{x} = \frac{\partial \mathbf{h}}{\partial x}\mathbf{f}(x) + \frac{\partial \mathbf{h}}{\partial x}\mathbf{g}(x)\tau = L_{\mathbf{f}}\mathbf{h}(x) + L_{\mathbf{g}}\mathbf{h}(x)\tau = \dot{\theta} \quad (5)$$

and

$$\ddot{y} = L_{\mathbf{f}}^2\mathbf{h}(x) + L_{\mathbf{g}}L_{\mathbf{f}}\mathbf{h}(x) = \frac{\partial L_{\mathbf{f}}h}{\partial x}\mathbf{f}(x) + \frac{\partial L_{\mathbf{f}}h}{\partial x}\mathbf{g}(x)\tau.$$

It may be noted that the input τ appears in the second derivative of the output $\ddot{y}$. Choosing a dynamic state feedback based control input of the form

$$\tau \triangleq \frac{-L_{\mathbf{f}}^{\rho}\mathbf{h}(x) + u}{L_{\mathbf{g}}L_{\mathbf{f}}^{\rho-1}\mathbf{h}(x)}, = -\frac{\sigma_a.\sigma_b}{\sigma_c}, \quad (6)$$

we obtain

$$\ddot{y} = u, \quad (7)$$

such that output y is linear in terms of control input u. Similar analysis is possible in case ϕ is chosen as the output. Note that, $\sigma_a = 8\ell_1{}^2\ell_2 m_1 + 24\ell_1{}^2\ell_2 m_2 + 8\ell_2{}^3 m_2 \sin^2\phi - 18\ell_1{}^2\ell_2 m_2 \cos^2\phi$, $\sigma_b = (8\ell_1{}^2 m_1 + 24\ell_1{}^2 m_2 + 8\ell_2{}^2 m_2 - 18\ell_1{}^2 m_2 \cos^2\phi -$

$8\ell_2{}^2 m_2 \cos^2\phi)u + 6g\ell_1 m_1 \sin\theta + 12g\ell_1 m_2 \sin\theta - 12\ell_1\ell_2 m_2 \dot{\phi}^2 \sin\phi + 6g\ell_2 m_2 \cos\theta \sin\phi - 9g\ell_1 m_2 \cos^2\phi \sin\theta + 16\ell_2{}^2 m_2 \dot{\phi}\dot{\theta}\cos\phi\sin\phi + 12\ell_1\ell_2 m_2 \dot{\theta}^2 \cos^2\phi \sin\phi$, and $\sigma_c = 9\ell_1\cos\phi\left(8\ell_1{}^2 m_1 + 24\ell_1{}^2 m_2 + 8\ell_2{}^2 m_2 - 9\ell_1\cos\phi\right) - 9\ell_1\cos\phi\left(18\ell_1{}^2 m_2 \cos^2\phi 9\ell_1\cos\phi\right) - 9\ell_1\cos\phi\left(8\ell_2{}^2 m_2 \cos^2\phi\right)$. Clearly, at $\phi = \pm\frac{\pi}{2}k$, $k \in \mathbb{N}$, $\cos\phi = 0$ and therefore $\sigma_c = 0$. To avoid this singularity, for practical purposes, $\tau = \sigma_c{}^\dagger \sigma_a \sigma_b$ may be used, so that $\sigma_c{}^\dagger = 0$, when $\cos\phi = 0$. Note that $(\cdot)^\dagger$ denotes the Moore-Penrose generalized inverse.

In an ideal situation, τ may be used for tracking trajectories on θ by specifying u as

$$u = \ddot{\theta}_{\text{desired}}, \tag{8}$$

when the reference command θ_{desired} is sufficiently smooth. The resultant tracking behavior is shown in Fig. 3, which also depicts the inputs τ and u.

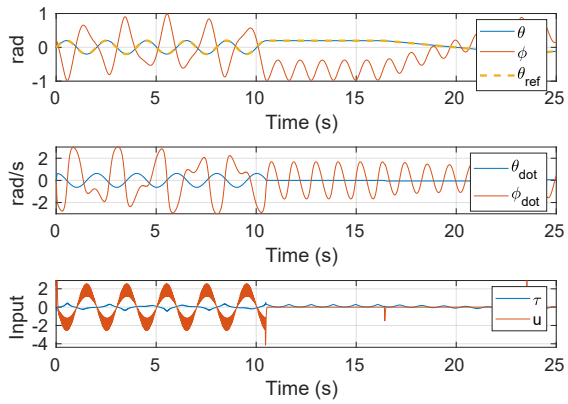

Fig. 3. Simulated tracking behavior using non-linear state feedback that linearizes the output θ with the help of input (6) based on the relative degree of the system shows that the reference commands on θ are tracked by choosing the auxiliary control input $u = \ddot{\theta}_{\text{ref}}$. Similar linearizing control inputs can be derived for ϕ.

Fact 3.1: Let $\mathcal{D}_\rho = \left\{x \in \mathbb{R}^4 | \phi = \pm\frac{\pi}{2}k, k \in \mathbb{N}\right\}$. Then the swirling pendulum system with $y = \mathbf{h}(x) = \theta$ as output has a relative degree $\rho = 2$ in the region $\mathbb{R}^4 - \mathcal{D}_\rho$.

Fact 3.1 may be appreciated by noting that control input τ appears in the second derivative of output θ and is multiplied by the term $9\ell_1\cos\phi$ and output $y = \theta$ does not depend on input τ for all ϕ, that cause $9\ell_1\cos\phi = 0$. This means, swirling pendulum system with θ as output does not have a well defined relative degree in the region $\mathcal{D}_\rho$.

Next, we discuss the collocated and non-collocated partial feedback linearization for tracking commands on ϕ and θ respectively.

B. Partial Feedback Linearization

1) Collocated Partial Feedback Linearization to Track Commands on ϕ: Equation (1) may be rewritten as

$$\mathbf{M}_{11}\ddot{\theta} + \mathbf{M}_{12}\ddot{\phi} + \mathbf{C}_{11}\dot{\theta} + \mathbf{C}_{12}\dot{\phi} + \mathbf{G}_1 = 0, \tag{9}$$

and

$$\mathbf{M}_{21}\ddot{\theta} + \mathbf{M}_{22}\ddot{\phi} + \mathbf{C}_{21}\dot{\theta} + \mathbf{C}_{22}\dot{\phi} + \mathbf{G}_2 = \tau, \tag{10}$$

and from (9), we have

$$\ddot{\theta} = -\mathbf{M}_{11}{}^{-1}(\mathbf{M}_{12}\ddot{\phi} + \mathbf{C}_{11}\dot{\theta} + \mathbf{C}_{12}\dot{\phi} + \mathbf{G}_1). \tag{11}$$

It is easy to establish that $\mathbf{M}_{11} \neq 0$ for all $x \in \mathbb{R}^4$, and $\mathbf{M}_{11}{}^{-1}$ exists for all $x \in \mathbb{R}^4$. Substituting (11) in (10), we have

$$\tau = \mathbf{G}_2 - \mathbf{M}_{11}{}^{-1}\mathbf{M}_{12}\mathbf{G}_1 + \left(\mathbf{M}_{22} - \mathbf{M}_{21}\mathbf{M}_{11}{}^{-1}\mathbf{M}_{12}\right)\ddot{\phi} + \begin{bmatrix}\mathbf{C}_{21} - \mathbf{M}_{11}{}^{-1}\mathbf{M}_{12}\mathbf{C}_{21} & \mathbf{C}_{22} - \mathbf{M}_{11}{}^{-1}\mathbf{M}_{12}\mathbf{C}_{21}\end{bmatrix}\begin{bmatrix}\dot{\theta}\\ \dot{\phi}\end{bmatrix}. \tag{12}$$

Therefore, choosing τ as

$$\tau = \mathbf{G}_2 - \mathbf{M}_{11}{}^{-1}\mathbf{M}_{12}\mathbf{G}_1 + \left(\mathbf{M}_{22} - \mathbf{M}_{21}\mathbf{M}_{11}{}^{-1}\mathbf{M}_{12}\right)u + \begin{bmatrix}\mathbf{C}_{21} - \mathbf{M}_{11}{}^{-1}\mathbf{M}_{12}\mathbf{C}_{21} & \mathbf{C}_{22} - \mathbf{M}_{11}{}^{-1}\mathbf{M}_{12}\mathbf{C}_{21}\end{bmatrix}\begin{bmatrix}\dot{\theta}\\ \dot{\phi}\end{bmatrix}, \tag{13}$$

with an user-defined auxiliary input u and substituting in (12) results into

$$\ddot{\phi} = u. \tag{14}$$

This allows the use of choosing auxiliary input u as $u = \ddot{\phi}_{\text{desired}}$ to follow a desired trajectory on ϕ. Fig. 4 shows the simulation results for tracking reference commands on ϕ using colloacted partial feedback linearization.

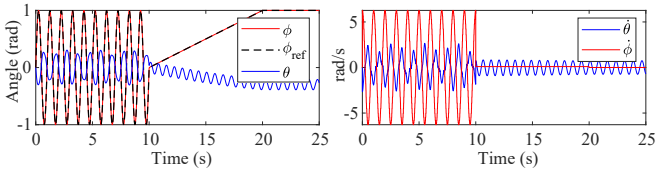

Fig. 4. Simulations depicting collocated partial feedback linearization showing tracking of a desired trajectory for ϕ. The control law (13) linearizes the dynamics of the coordinate ϕ and auxiliary control input chosen as $u = \ddot{\phi}_{\text{desired}}$ allows tracking of desired reference trajectory ϕ_{ref}.

2) Non-Collocated Partial Feedback Linearization to Track Commands on θ: From (9), we have

$$\ddot{\phi} = -\mathbf{M}_{12}{}^{\dagger}(\mathbf{M}_{11}\ddot{\theta} + \mathbf{C}_{11}\dot{\theta} + \mathbf{C}_{12}\dot{\phi} + \mathbf{G}_1). \tag{15}$$

Note the use of Moore-Penrose generalized inverse above, to accommodate the possibility of $\mathbf{M}_{12} = 0$ when $\cos\phi$ is zero. Substituting (15) in (10) we have

$$\tau = \mathbf{G}_2 - \mathbf{M}_{12}{}^{\dagger}\mathbf{M}_{22}\mathbf{G}_1 + \left(\mathbf{M}_{21} - \mathbf{M}_{22}\mathbf{M}_{21}{}^{\dagger}\mathbf{M}_{11}\right)\ddot{\theta} + \begin{bmatrix}\mathbf{C}_{21} - \mathbf{M}_{22}\mathbf{M}_{12}^{\dagger}\mathbf{C}_{11} & \mathbf{C}_{22} - \mathbf{M}_{22}\mathbf{M}_{12}^{\dagger}\mathbf{C}_{12}\end{bmatrix}\begin{bmatrix}\dot{\theta}\\ \dot{\phi}\end{bmatrix}. \tag{16}$$

Choosing τ as

$$\tau = \mathbf{G}_2 - \mathbf{M}_{12}{}^{\dagger}\mathbf{M}_{22}\mathbf{G}_1 + \left(\mathbf{M}_{21} - \mathbf{M}_{22}\mathbf{M}_{21}{}^{\dagger}\mathbf{M}_{11}\right)u + \begin{bmatrix}\mathbf{C}_{21} - \mathbf{M}_{22}\mathbf{M}_{12}^{\dagger}\mathbf{C}_{11} & \mathbf{C}_{22} - \mathbf{M}_{22}\mathbf{M}_{12}^{\dagger}\mathbf{C}_{12}\end{bmatrix}\begin{bmatrix}\dot{\theta}\\ \dot{\phi}\end{bmatrix} \tag{17}$$

with an user-defined auxiliary input u and substituting in (12) results into

$$\ddot{\theta} = u. \tag{18}$$

This allows the use of choosing auxiliary input u as $u = \ddot{\theta}_{\text{desired}}$ to follow a desired trajectory on θ. Fig. 5 shows the simulation results for tracking reference commands on θ

using non-colloacted partial feedback linearization.

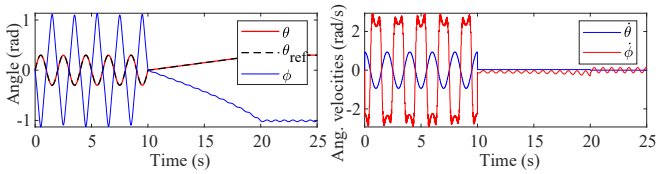

Fig. 5. Simulations depicting non-collocated partial feedback allowing perfect tracking of a desired trajectory on θ. One important point to consider here is that we can only track reference commands having an angular displacement within the range $[-0.3, 0.3]$ rad. This is because we are able to produce a holding torque for values of θ within the range $[-\tilde{\theta}_e \ \tilde{\theta}_e]$. Although it is possible to reach values of θ beyond this range, the holding torque required maintain these system states does not exist and cannot be determined [1, Fact1].

IV. Internal/Zero Dynamics of the Swirling Pendulum

For output $\mathbf{h}(x) = \theta$, swirling pendulum has a relative degree $\rho = 2 \neq n$, which implies the presence of zero dynamics. In order to analyse the behavior of the zero dynamics, we first define a change of state variables $z \triangleq T(x)$, where

$$z = T(x) = \begin{bmatrix} \Phi_1(x) \\ \Phi_2(x) \\ \mathbf{h}(x) \\ L_f\mathbf{h}(x) \end{bmatrix} = \begin{bmatrix} \eta \\ \xi \end{bmatrix} = \begin{bmatrix} \Phi_1 \\ \Phi_2 \\ \theta \\ \dot{\theta} \end{bmatrix} \tag{19}$$

and $T(\cdot)$ is a diffeomorphism. Choosing $\Phi_1(x) = \dot{\theta} - \mathbf{g}_3\mathbf{g}_4^{-1}\dot{\phi}$ and $\Phi_2(x) = \phi$ to satisfy

$$\frac{\partial \Phi_k}{\partial x}\mathbf{g}(x) = 0 \qquad \text{for } 1 \leq k \leq (n-\rho),\ x \in \mathbb{R}^4, \tag{20}$$

we have $T = \begin{bmatrix} 0 & 0 & 1 & -\frac{\mathbf{g}_3}{\mathbf{g}_4} \\ 0 & 1 & 0 & 0 \\ 1 & 0 & 0 & 0 \\ 0 & 0 & 1 & 0 \end{bmatrix}$ and $z = \begin{bmatrix} \dot{\theta} - \frac{\mathbf{g}_3\dot{\phi}}{\mathbf{g}_4} \\ \phi \\ \theta \\ \dot{\theta} \end{bmatrix}$. Furthermore, $\Phi = \begin{bmatrix} \dot{\theta} - \frac{\mathbf{g}_3\dot{\phi}}{\mathbf{g}_4} \\ \phi \end{bmatrix}$ and $\frac{\partial \Phi}{\partial x} = \begin{bmatrix} 0 & 0 & 1 & -\frac{\mathbf{g}_3}{\mathbf{g}_4} \\ 0 & 1 & 0 & 0 \end{bmatrix}$. The internal dynamics of the swirling pendulum system is then given by

$$\dot{\eta} = \frac{\partial \Phi}{\partial x}\dot{x} = \frac{\partial \Phi}{\partial x}\mathbf{f}(x) = \begin{bmatrix} f_3 - \mathbf{g}_3\mathbf{g}_4^{-1}f_4 \\ f_2 \end{bmatrix}.$$

The normal form equations of the swirling pendulum having θ as the output are given by

$$\dot{\eta} = \begin{bmatrix} f_3 - \mathbf{g}_3\mathbf{g}_4^{-1}f_4 \\ f_2 \end{bmatrix} = f_{\text{internal}}(\eta, \xi), \tag{21}$$

$$\dot{\xi} = A_{\text{ccf}}\xi + B_{\text{ccf}}(L_gL_f\mathbf{h}(x))^{-1}(-L_f\mathbf{h}(x) + u), \tag{22}$$

and

$$y = C_{\text{ccf}}\xi, \tag{23}$$

where $\eta = \begin{bmatrix} \dot{\theta} - \frac{\mathbf{g}_3\dot{\phi}}{\mathbf{g}_4} \\ \phi \end{bmatrix}$, $\xi = \begin{bmatrix} \theta \\ \dot{\theta} \end{bmatrix}$, $A_{\text{ccf}} = \begin{bmatrix} 0 & 1 \\ 0 & 0 \end{bmatrix}$, $B_{\text{ccf}} = \begin{bmatrix} 0 \\ 1 \end{bmatrix}$ and $C_{\text{ccf}} = \begin{bmatrix} 1 & 0 \end{bmatrix}$. Equations (22) and (23) represent the linearized part of the swirling pendulum system. The full symbolic expressions for the system in the normal form are very long and therefore not stated. For practical purposes, numerical values may be substituted making use of a symbolic computation software package. Substituting $\xi = 0$ in $f_{\text{internal}}(\eta, \xi)_{\text{ at } \zeta=0} = f_{\text{zero}}(\eta)$, we arrive at the expression for zero dynamics of the swirling pendulum given by

$$f_{\text{zero}}(\eta) = \begin{bmatrix} \frac{4}{3}m_2^2\ell_2^3 g\sin\phi - 2\frac{\mathbf{M}_{21}}{\mathbf{M}_{11}}m_2\ell_1\ell_2\cos\phi \\ \dot{\phi} \end{bmatrix}. \tag{24}$$

V. Inversion-based Tracking Control of the Swirling Pendulum while avoiding Non-minimum Phase Zeros

In this section, we discuss a discrete-time inversion based tracking control scheme for tracking desired trajectories on the system outputs of the swirling pendulum. We define for control design, the system matrices $A_d \triangleq (At_s + I_n)$ and $B_d \triangleq Bt_s$, where A and B are linearized matrices for the swirling pendulum from [1] based on parameter values in Table (II) for state vector $x^\intercal = \begin{bmatrix} \theta & \phi & \dot{\theta} & \dot{\phi} \end{bmatrix}^\intercal$ at equilibrium point $x_e^\intercal = \begin{bmatrix} 0 & 0 & 0 & 0 \end{bmatrix}^\intercal$ and t_s is the sampling time. The feedforward inversion based control schemes discussed in [8] or [9] may not be used with the choice of positions θ or ϕ as outputs, since the systems with these outputs will have linearizations containing a pair of zeros on the imaginary axis or the unit circle resulting in an unstable feedforward controller. Instead we choose all the four states as the outputs $y \triangleq C_dx$, where $C_d \triangleq \begin{bmatrix} 1 & 0 & 0 & 0 \\ 0 & 1 & 0 & 0 \\ 0 & 0 & 1 & 0 \\ 0 & 0 & 0 & 1 \end{bmatrix}$ that results into a single-input multi-output system with one input and four outputs having no system zeros given by

$$x_{k+1} = A_dx_k + B_du_k \tag{25}$$

and

$$y_k = C_dx_k. \tag{26}$$

Note that, k is a sampled-time index. Tracking arbitrary reference commands simultaneously on four outputs using one control input is not possible. For this discrete-time LTI system representation having no system zeros, we choose the selective tracking inversion based control scheme described in [7] that uses time varying weighting matrices W_k and V_k in the control input given by

$$u_k = \left((\tilde{C}_dB_d)^\intercal W_{k+1}(\tilde{C}_dB_d) + V_k\right)^\dagger (\tilde{C}_dB_d)^\intercal W_{k+1}{}^\intercal \left(\tilde{y}_{\text{ref},k+1} - \tilde{C}_dA_dx_k\right), \tag{27}$$

to prioritize tracking of output components for systems having more number of outputs than inputs. Also note that, $W \in \mathbb{R}^{l\times l}$ and $V \in \mathbb{R}^{m\times m}$ are positive semi-definite matrices chosen by the user to determine the component-wise priority of tracking outputs or usage of control inputs respectively. m and l are the number of input and output components respectively. We choose $V = 0$ in the following discussion for simplicity and demonstrate the effects of choosing different values of W on the tracking performance. Furthermore, to simplify the choice of entries in W matrix, we choose W to be a diagonal matrix having diagonal entries $W_{11} = w_\theta$, $W_{22} = w_\phi$ and $W_{33} = w_{\dot{\theta}}$ $W_{44} = w_{\dot{\phi}}$ corresponding to components θ, ϕ, $\dot{\theta}$ and $\dot{\phi}$.

Let $Q(j,:)$ represent the j^{th} row of matrix Q. Then we may define a matrix $\tilde{C}_d$ that accounts for input-output delays

on account of relative degree as

$$\tilde{C}_d \triangleq \begin{bmatrix} C_d(1,:)A_d \\ C_d(2,:)A_d \\ C_d(3,:) \\ C_d(4,:) \end{bmatrix}, \tag{28}$$

following the relative degree vector definition (Definition 3.1) in [7]. Also, $\tilde{y}_{\text{ref},k+1} = \begin{bmatrix} \tilde{y}_{\text{ref},k+1}(1,:) \\ \tilde{y}_{\text{ref},k+1}(2,:) \\ \tilde{y}_{\text{ref},k+1}(3,:) \\ \tilde{y}_{\text{ref},k+1}(4,:) \end{bmatrix} \triangleq \begin{bmatrix} y_{\text{ref},k+3}(1,:) \\ y_{\text{ref},k+3}(2,:) \\ y_{\text{ref},k+1}(3,:) \\ y_{\text{ref},k+1}(4,:) \end{bmatrix}$ represents the previewed reference command to account for the input-output delay due to relative degree of the system.

By choosing sampling time interval $t_s = 0.001$ s and parameters listed in Table II, we simulate tracking control using control action (27) for swirling pendulum system nonlinear equations of motion having all four states as outputs for a time range of 0 to 120 seconds with weighting matrix W chosen as

1) 0 to 24 seconds: $w_\theta = 10$, $w_\phi = w_{\dot\theta} = w_{\dot\phi} = 0.0001$,
2) 24 to 48 seconds: $w_\phi = 10$, $w_\theta = w_{\dot\theta} = w_{\dot\phi} = 0.0001$,
3) 48 to 72 seconds: $w_\theta = 10$, $w_\phi = 2$, $w_{\dot\theta} = w_{\dot\phi} = 0.0001$,
4) 72 to 96 seconds: $w_{\dot\theta} = 20$, $w_\theta = w_\phi = w_{\dot\phi} = 0.1$,
5) 96 to 120 seconds: $w_{\dot\phi} = 20$, $w_\theta = w_\phi = w_{\dot\theta} = 0.1$.

Larger weights indicate higher priority for tracking. The simulation results are shown in Fig. 6. Between time ranges 0-24, 24-48, 72-96 and 96-120 seconds θ, ϕ, $\dot\theta$ and $\dot\phi$ respectively are tracked on priority specified by weights in W associated with these components. The problem of non-minimum phase zeros while tracking outputs is thus avoided by using all the states as the output vector and the control input (27) for selectively tracking the desired output.

VI. Conclusion

We presented in this paper some properties of the swirling pendulum mechanism along with its feedback linearization, zero dynamics and the control problem of prioritized inversion-based control. The presented results demonstrate the utility of the swirling pendulum as a pedagogical tool to explain several concepts and phenomena in dynamics, systems and control. Approaches like geometric control, Hamiltonian based formulation and damping injection for stabilization [6] are naturally suited for the swirling pendulum. The future work constitutes experiments on a hardware setup to demonstrate swing-up and stabilizing control of the swirling pendulum.

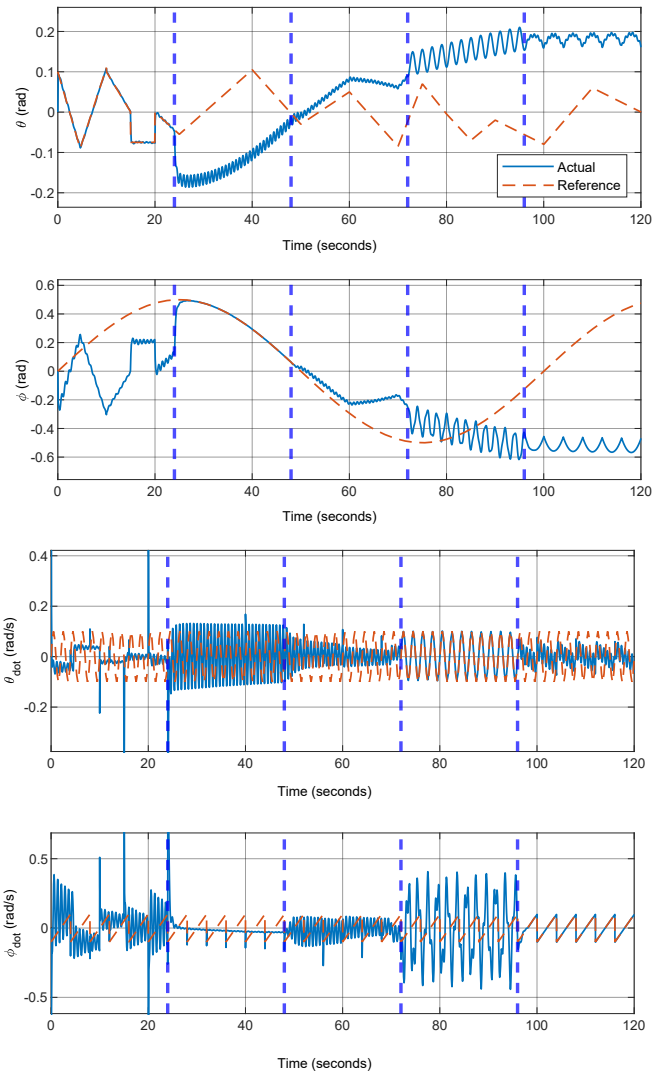

Fig. 6. Simulation results depict the tracking of individual output components selectively based on choice of weighting terms w_θ, w_ϕ, $w_{\dot\theta}$ and $w_{\dot\phi}$ corresponding to respective state/output contained in matrix W, using control input (27). When the weighting terms for a certain state/output are chosen to be reasonably higher than other weighting terms tracking controller assigns higher priority for that output and enables the output to closely follow its desired reference command. When priorities/weights chosen for multiple outputs are relatively similar to each other, a compromise in tracking performance is reached.

References

[1] S. D. Kadam, U. Shah, A. D'Souza, P. G. Shanthamurthy, N. Raj, R. N. Banavar, and H. J. Palanthandalam-Madapusi, "The swirling pendulum: conceptualization, modeling, equilibria and control synthesis," in *Dynamic Systems and Control Conference*, vol. 84270, p. V001T16A002, American Society of Mechanical Engineers, 2020.

[2] M. W. Spong, "The swing up control problem for the acrobot," *IEEE control systems*, vol. 15, no. 1, pp. 49–55, 1995.

[3] M. W. Spong and D. J. Block, "The pendubot: A mechatronic system for control research and education," in *Decision and Control, 1995., Proceedings of the 34th IEEE Conference on*, vol. 1, pp. 555–556, IEEE, 1995.

[4] K. Furuta, M. Yamakita, and S. Kobayashi, "Swing up control of inverted pendulum," in *Industrial Electronics, Control and Instrumentation, 1991. Proceedings. IECON'91., 1991 International Conference on*, pp. 2193–2198, IEEE, 1991.

[5] O. Boubaker, "The inverted pendulum: A fundamental benchmark in control theory and robotics," in *Education and e-Learning Innovations (ICEELI), 2012 international conference on*, pp. 1–6, IEEE, 2012.

[6] R. Ortega, M. W. Spong, F. Gómez-Estern, and G. Blankenstein, "Stabilization of a class of underactuated mechanical systems via interconnection and damping assignment," *IEEE transactions on automatic control*, vol. 47, no. 8, pp. 1218–1233, 2002.

[7] S. D. Kadam, A. Rao, B. Prusty, and H. J. Palanthandalam-Madapusi, "Selective tracking using linear trackability analysis and inversion-based tracking control," in *2020 American Control Conference (ACC)*, pp. 5346–5351, IEEE, 2020.

[8] Q. Zou and S. Devasia, "Preview-based stable-inversion for output tracking," in *American Control Conference (ACC)*, vol. 5, pp. 3544–3548, IEEE, 1999.

[9] K. George, M. Verhaegen, and J. M. Scherpen, "Stable inversion of MIMO linear discrete time nonminimum phase systems," in *Proc. 7th Mediterranean Conference on Control and Automation*, pp. 267–281, 1999.